



UKAEA

Preprint



Loar.

TEARING MODE STABLE DIFFUSE PINCH CONFIGURATIONS

D C ROBINSON

CULHAM LABORATORY
Abingdon Oxfordshire

1977

This document is intended for publication in a journal or at a conference and is made available on the understanding that extracts or references will not be published prior to publication of the original, without the consent of the authors.

Enquiries about copyright and reproduction should be addressed to the Librarian, UKAEA, Culham Laboratory, Abingdon, Oxfordshire, England

TEARING MODE STABLE DIFFUSE PINCH CONFIGURATIONS

D C Robinson

Culham Laboratory, Abingdon, Oxon., OX14 3DB, U.K.
(Euratom/UKAEA Fusion Association)

ABSTRACT

It is demonstrated that tearing mode stable diffuse pinch configurations of the reverse field pinch type exist at zero β for a current carrying column surrounded by a small vacuum region. The conducting wall plays a vital role in this stability both to $m = 0$ and $m = 1$ modes. The core of the plasma, which has to satisfy a limiting resistive stability criterion, is of the form given by Taylor for a minimum energy state but the outer region is quite different. Values of the pinch configuration parameter θ up to 3 are possible permitting strong ohmic heating with low current densities near the wall. Such configurations can be stable to ideal hydromagnetic modes for central values of β of $\sim 15\%$.

(Submitted for publication in Nuclear Fusion)

I. Introduction

The hydromagnetic stability of the diffuse linear pinch has been discussed by many authors, [1,2,3,4,5,6]. This has yielded potential magnetic configurations which can be magnetohydrodynamically stable at significant values of β . These include the tokamak, [4], the screw pinch [6] and the reverse field pinch [5]. All these configurations exhibit to some degree kink modes in the experimental devices even when the conditions for ideal hydromagnetic stability are satisfied. The finite conductivity kink mode or tearing mode has been discussed as the explanation for these residual instabilities, [7,8,9]. To a good approximation the analysis of such modes can be carried out in cylindrical geometry [4] but there are important stabilising effects from toroidal curvature in the case of a tokamak [10]. Indeed other effects such as radial flow [11,12], finite dissipation, for example viscosity [13,14], all have a stabilising influence on a real plasma in which the magnetic Reynolds number or Lundquist number - $S = \tau_\sigma / \tau_H$ (τ_σ is the field diffusion time and τ_H the Alfvén transit time) is finite. Present pinch experiments have values of S (with respect to the poloidal field) which range between 10^2 and 10^6 . This number as well as being related to the growth rate of resistive modes also controls the degree to which a pinch can relax by field line re-connection [15,16,17,18]. This relaxation can occur via tearing modes which saturate in amplitude [19]. Naturally one would therefore expect that diffuse pinch configurations which are tearing mode stable to be important. They represent a form of lower energy state to which a pinch might relax if the practical constraints permitted such a configuration. A well known example of this is the force-free Bessel function model configuration for a cylindrical pinch which has been shown to be a minimum energy state by Taylor [16]. Such a configuration has the cylindrical tearing mode driving term $\frac{d}{dr} \left(\frac{\underline{J} \cdot \underline{B}}{B^2} \right)$ exactly equal to zero (\underline{J} is the current density and \underline{B} the magnetic field) which is unlikely to be true in practice. In the cylindrical tokamak this term is approximately $\frac{dJ}{dr} \frac{z}{r}$ and so a uniform current distribution is required to avoid resistive instabilities and the resultant relaxation.

A more realistic constraint on the current distribution is that the current should be small or zero at some outer surface. In a pinch device this could arise from

- (i) surface phenomena and impurities giving low temperatures near the outer surface;
- (ii) field line errors which make it possible to maintain only low temperatures near the outer boundary because of heat conduction along the field lines to the wall;
- (iii) inability to control the equilibrium precisely enough which permits 'scrape off' of the outer layers of the plasma;
- (iv) the existence of a magnetic aperture, material limiter or a metal liner.

We therefore conclude that in pinch devices the parallel current gradient cannot be zero everywhere and so it is important to establish if there are any tearing mode stable diffuse pinch configurations in this case.

For the tokamak, optimised current profiles have been obtained [20] which do permit stability to all resistive kink modes. In this case only a few singular surfaces associated with $q(r) = \frac{rB_z}{RB_\theta} = \frac{m}{n}$, (with m, n the poloidal and toroidal mode numbers which are small) are important and tailoring the current gradient in these regions permits stable current profiles to be obtained for $q(a) \sim 2.5$ without a conducting wall. Configurations resembling those of a screw pinch are obtained for $q(a) \sim 1.5$ if a conducting wall is placed close to the edge of the plasma.

In the diffuse pinch a similar problem has been investigated [21,22] where $m = 1$ and $m = 0$ are the dominant modes. In this case the possible singular surfaces are very closely spaced as $q \ll 1$ and the problem is best considered as a continuum of surfaces for all of which we require stability. The analysis we shall perform is essentially the analogue of that of Newcomb, as applied to a diffuse pinch which is slightly resistive [23,24].

We first discuss the basic equations and the limitations imposed by on-axis criteria in Section II. The method of solution is described in Section III.

Results for various well known pinch configurations are presented in Section IV. In Section V we obtain an 'optimised' reverse field pinch configuration and demonstrate that a small vacuum region outside the pinch can still give stability. In Section VI brief mention is made of the stability of such configurations at finite β . Finally we discuss the relevance of the result on tearing mode stability to reverse field pinches and to a lesser extent to tokamaks and screw pinches.

II. Tearing modes in cylindrical geometry and on axis stability criteria

We consider a cylindrically symmetric plasma with axial magnetic field $B_z(r)$, azimuthal magnetic field $B_\theta(r)$ and scalar plasma pressure $p(r)$. The equilibrium condition is

$$\frac{dp}{dr} + B_z \frac{dB_z}{dr} + \frac{B_\theta}{r} \frac{d}{dr} r B_\theta = 0 \quad \dots (1)$$

A radial magnetic field perturbation of the form $B_r = b_r(r) \exp(im\theta + ikz + \omega t)$ is considered and for large but finite conductivity satisfies the equation

$$\frac{d^2\psi}{dr^2} + A\psi = 0 \quad \dots (2)$$

where $\psi = \frac{r^{3/2} b_r(r)}{(m^2 + K^2 r^2)^{1/2}}$ and

$$\begin{aligned} -A = & \frac{m^2 + K^2 r^2}{r^2} - \sigma^2 + \frac{d\sigma}{dr} \frac{(mB_z - Kr B_\theta)}{mB_\theta + Kr B_z} - \frac{2\sigma mK}{m^2 + K^2 r^2} - \frac{(m^4 + 10 m^2 K^2 r^2 - 3K^4 r^4)}{4r^2(m^2 + K^2 r^2)^2} \\ & + \frac{2K^2 r}{(mB_\theta + Kr B_z)^2} \frac{dp}{dr} - \frac{d}{dr} \left(\frac{1}{B^2} \frac{dp}{dr} \right) + \left(\frac{1}{B^2} \frac{dp}{dr} \right)^2 - \frac{(m^2 - K^2 r^2)}{m^2 + K^2 r^2} \frac{1}{rB^2} \frac{dp}{dr} \\ & - \frac{2}{B^2} \frac{dp}{dr} \frac{1}{mB_\theta + Kr B_z} [\sigma(mB_z - Kr B_\theta) + KB_z - \frac{mB_\theta}{r}] \quad \sigma = \frac{J \cdot B}{B^2} \end{aligned}$$

except close to the singular surface r_s where $F = \frac{mB_\theta}{r} + K B_z = 0$. In this region a higher order finite resistivity equation must be used. Here we will let $\frac{dp}{dr} \rightarrow 0$ and thereby remove any pressure driven effects on the tearing modes. To determine the tearing mode stability we solve equation (2) through the

singular surface r_s with the appropriate boundary condition at $r = 0$, $\psi \propto r^{m+1/2}$ to determine the point at which $\psi = 0$. This will represent the position of a perfectly conducting wall to give marginal stability to the mode under investigation. The more usual way in which the problem is posed[8] is to solve for the derivative, $\frac{d\psi}{dr}$ on both sides of the singular surface with an assumed wall position where $\psi = 0$, and then calculate

$$\Delta' = \frac{\left. \frac{d\psi}{dr} \right|_{+\epsilon} - \left. \frac{d\psi}{dr} \right|_{-\epsilon}}{\psi(r_s)} \quad \dots (3)$$

Finite resistivity analysis[25,26,27] shows that the condition for instability is $\Delta' > 0$ with growth rate given by

$$W = 0.55 (\Delta')^{4/5} \left(\frac{\eta}{4\pi} \right)^{3/5} \left(\frac{dF}{dr} \right)^{2/5} / (4\pi\rho)^{1/5} \quad \dots (4)$$

where η is the resistivity, ρ the density and $\frac{dF}{dr}$ is evaluated at the singular surface. At values of S attainable in many experiments the actual calculated value of W [13,14] falls short of the asymptotic value given in (4) which is valid in the limit $S \rightarrow \infty$. As we have already noted the criterion $\Delta' > 0$ is affected by pressure gradient and toroidal curvature effects[10], radial flow[11,12], viscosity[14] etc.

Our equation (2) is dominated by the singular term $\frac{1}{r} \frac{d\sigma}{dr} \frac{(mB_z - KrB\theta)}{F}$ which in the tokamak limit ($B_z \gg B_\theta$) becomes $\frac{1}{r} \frac{dJ_z}{dr} \cdot \frac{1}{F}$. It is this term which principally determines the tearing mode behaviour of the pinch. It should be noted that we obtain a solution for ψ which has a continuous behaviour across the singular surface. This implies that the plasma displacement ξ_r is singular at r_s however this is possible as the finite resistivity equations applicable in the region of r_s make ξ_r finite. This is the same behaviour as for the kink mode where r_s is in a vacuum region. Thus the tearing mode moves over smoothly into the kink mode at the edge of the plasma.

As the singularity approaches the origin it is possible to obtain a stability criterion from (2). In addition if the value of K is chosen so that

the value of F is small and positive then (2) is not singular but can give rise to oscillatory behaviour associated with ideal hydromagnetic instabilities arising from the curvature of the pitch. As has been shown previously [5,28] this curvature must satisfy for ideal hydromagnetic stability

$$\gamma = \frac{P}{2} \frac{d^2 P}{dr^2} \bigg|_{r \rightarrow 0} < - \frac{4}{8 + m^2} \quad \text{or } \gamma > 0 \quad (m \neq 0) \quad \dots (5)$$

- where the appropriate toroidal correction has also been given [28] and $P = qR$ (for $q < 1$ the correction is small). As $r_s \rightarrow 0$ equation (2) can be transformed to a form of the hypergeometric equation for which the product $r_s \Delta'$ can be calculated [29]. This is

$$r_s \Delta' \big|_{r_s \rightarrow 0} = -2\pi\Lambda \cot \pi |\chi| + 2\Lambda \left(\frac{1}{\chi} + \frac{1}{|\chi|} \right) \quad \dots (6)$$

where $\Lambda = \frac{1 + 2\gamma}{\gamma}$, $\chi = \frac{m}{2} - \left(\frac{m^2}{4} + \Lambda \right)^{\frac{1}{2}}$. The condition that χ be real corresponds to the criterion given in equation (5). We therefore obtain from (6) the on axis tearing mode stability criterion

$$\gamma > - \frac{4}{7 - 2m} \quad (m \neq 0) \quad \dots (7)$$

Thus for the $m = 1$ mode to be both stable to hydromagnetic and tearing modes as $r_s \rightarrow 0$ requires from (5) and (7)

$$-\frac{4}{9} > \gamma > -\frac{4}{5} \quad \dots (8)$$

i.e. the pitch, P , or q must decrease sufficiently rapidly as one moves away from the axis. This implies directly that the axial current must be peaked on axis for stability ($\gamma = -1$ is a flat axial current distribution) however $\frac{d\sigma}{dr}$ can have either sign. If the current is peaked on axis in a tokamak $\gamma > 0$ and then (7) can only be satisfied if $m \geq 4$ with $\gamma > 4$ for $m = 4$. As we have $nq(0) + m = 0$ on axis then $q(0) > 3$ or $q(0) \neq 3, 2, 1.5, \dots$ to satisfy (7). If the current distribution is peaked off axis, ie $\gamma < 0$ then in principle (7) could be satisfied with $q(0) < 1$. However it should be noted that toroidal curvature effects markedly influence the hydromagnetic criterion (5) for $q(0) \geq 1$ in a stabilising direction and also influence criterion (7) [10].

It should be noted that some of the previously given [5] reverse field pinch configurations which are hydromagnetically stable violate the above tearing mode stability criterion.

III. Method of solution of the radial field equation

Initially equation (2) was solved by integrating from $r=0$ to $r=r_s$ where $\frac{d\psi}{dr}$ has a logarithmic singularity. In this region we obtain by expansion

$$\psi \sim A(1-g x \ln |x|) + B(x - \frac{g x^2}{2}) \quad \dots (9)$$

where $x = r - r_s$ and $g = \frac{d\sigma}{dr} \left(\frac{mB_z}{r} - KB_\theta \right) \Big|_{r_s}$. A and B are constants obtained by fitting equation (9) to the computed solution. By integrating forward from the other side of the singularity using the values of A and B the marginal stability position for the conducting wall could be obtained from the position where $\psi = 0$. This method was found to be not sufficiently accurate in general. This was partly associated with difficulties in finding an optimal matching point for the solution in certain cases and with the behaviour for small r_s . In some cases good convergence could not be obtained.

A method for solving equations of the type given in equation (2) was developed. We start with a comparison equation [30]

$$\frac{d^2 u}{dx^2} + Q(x) u = 0 \quad \dots (10)$$

where Q has the same kind of singularity at the same position as A and has known solutions $u_1(x)$, $u_2(x)$. Assuming that

$$\psi = \alpha(x) u_1(x) + \beta(x) u_2(x) \quad \dots (11)$$

the problem then reduces to obtaining the two unknown functions α , β . A further condition is needed which we take to be

$$\frac{d\alpha}{dx} u_1 + \frac{d\beta}{dx} u_2 = 0 \quad \dots (12)$$

From (2), (10), (11) and (12) we obtain the two equations for α and β

$$\begin{aligned} \frac{d\alpha}{dx} &= - \frac{u_2(x) (Q - A)\psi}{W_0} \\ \frac{d\beta}{dx} &= \frac{u_1(x) (Q - A)\psi}{W_0} \end{aligned} \quad \dots (13)$$

where W_0 is the Wronskian $u_1 \frac{du_2}{dx} - u_2 \frac{du_1}{dx}$. Hence the second order equation in ψ is reduced to two first order equations in α and β and by an appropriate choice of $Q(x)$ the singularity in ψ is avoided.

Now $A(x)$ can be expanded in the form

$$A(x) = \frac{G}{x} + G_1 + \dots \quad (14)$$

If we choose $u_1(x) = \frac{x}{1 + ax + bx^2}$

then $u_2(x) = u_1(x) \left[-\frac{1}{x} + 2a \ln |x| + (a^2 + 2b)x + abx^2 + \frac{b^2 x^3}{3} \right] \dots \quad (15)$

and for all x we have

$$\frac{d^2 u}{dx^2} = -2 \left[\frac{a}{x} + (3b - 2a^2) + R(x) \right] u \quad (16)$$

with $R(x) = \frac{(x(6a^3 - 16b) + x^2(4a^4 - 14b^2 - 2a^2b) + x^3(8a^3b - 14ab^2) + x^4(4a^2b^2 - 6b^3))}{(1 + ax + bx^2)^2}$

From (16) and (14) we have

$$a = \frac{G}{2} = -\frac{d\sigma}{dr} \frac{(mB_z - Kr B_\theta)}{2r \frac{dF}{dr}}$$

$$b = \frac{G^2 + G_1}{6}, \quad G_1 = -\frac{d\sigma}{dr} \left(m \frac{dB_z}{dr} - Kr \frac{dB_\theta}{dr} - KB_\theta \right) + \sigma^2 - \frac{(m^2 + K^2 r^2)}{r^2} \quad (17)$$

$$+ \frac{m^4 + 10m^2 K^2 r^2 - 3K^4 r^4}{4r^2(m^2 + K^2 r^2)^2} + \frac{2\sigma mK}{m^2 + K^2 r^2} - \left(\frac{d^2 \sigma}{dr^2} - \frac{d\sigma}{dr} \frac{1}{r} - \frac{d\sigma}{dr} \frac{d^2 F}{dr^2} / 2 \frac{dF}{dr} \right) \frac{(mB_z - Kr B_\theta)}{r \frac{dF}{dr}}$$

where G and G_1 are evaluated at r_s .

By this means we have ensured that $Q-A$ in (13) goes to zero linearly with x as we approach the singularity at $x = 0$, α and β can then be obtained to any degree of accuracy required after specifying the boundary conditions at $r = 0$. The method has one defect: if a and b are such that u_1 has a pole in the range of integration then it is necessary to stop the calculation of α and β before the pole is reached and by matching values and derivatives at this point (by high order interpolation) continue the forward integration of equation (2) in the normal way. The accuracy is not impaired by the presence of a pole if this is done.

The calculation uses a variable step length until the specified accuracy in the conducting wall position (e.g. 0.1%) is obtained.

The value of Δ' is easily obtained from the calculation as

$$\Delta' = \frac{\alpha|_{+\epsilon} - \alpha|_{-\epsilon}}{-\beta} \quad \dots (18)$$

The value of α is altered at the singularity subject to a specified Δ' and the resultant wall position obtained for which $\psi = 0$.

IV. Application to a variety of diffuse pinch configurations

In the first instance a variety of tokamak current distributions were investigated including the peaked, rounded and flattened models [8]. This was to compare the predictions for the wall position required to give marginal stability with previous results and to compare with the results of growth rate calculations [13] of the resistive tearing mode for an incompressible plasma performed with the help of the code RIP 4A [31]. In the light of these studies the current distributions were modified to match more closely the inferred current distributions in a number of devices with the current falling to zero in a smooth way at a specified edge of the plasma, and with a vacuum region existing out to a conducting wall. Both skin current distributions, possibly associated with the formation phase of the plasma, and reverse current distributions which occur in minor radius compression experiments [32] were investigated. As an example Fig.1 shows the radial field perturbations obtained from the marginal calculation presented here and that calculated for a growing mode close to marginal stability. This is for an $m = 2$ mode with a current distribution $J_z = J_{z0}(1-r^4)^2$ and the magnetic Reynolds number, $S = 10^4$, was sufficiently large that the resistive layer thickness was only a small fraction of the radius. The position of the singular surface is indicated. These growth rate calculations will be reported more fully elsewhere.

Turning now to pinch configurations we first investigate the force-free paramagnetic model [24, 33, 34] which compares well with some experiments [35]. This configuration has a current density which decreases to zero at large radii. The tearing mode stability of this model was first investigated by Kadomtsev [24] who calculated that the normalised wall radius for stability

was 2.8. (The normalised radius used in all the subsequent calculations is obtained by defining the axial field and current density on axis to be unity.) Fig.2 shows the marginal stability diagram obtained from our calculations for the $m = 1$ mode. Modes with $m = 0$ and $m \geq 2$ are stable. The diagram is plotted in the wavenumber, normalised radius plane and shows the position of the singular surface $F = 0$. For this model $\gamma = -\frac{1}{2}$ which satisfies equation (8) so no on axis tearing mode is present. If there is no singular surface ($K > -\frac{1}{2}$) then the position of the conducting wall is as given by the usual hydromagnetic analysis [35]. For $K < -\frac{1}{2}$ when a singularity exists in the plasma the behaviour of the MHD and tearing modes is quite different as indicated in the diagram. The MHD curve is obtained using the Newcomb analysis [23] which in this case makes the radial field perturbation at the singular surface zero and considers the plasma as made up of two separate domains, inside and outside the singular surface. In the tearing mode analysis the singular behaviour associated with $r = 3.16$ is removed and the maximum wall radius for stability is $R_c = 2.4527$. This radius is related to the pinch configuration parameter, θ , used in experiments where

$$\theta = \frac{B_\theta(r_{\text{wall}})}{B_{z0}} \quad \text{and} \quad B_{z0} = \frac{2}{r_w^2} \int_0^{r_w} B_z(r) r \, dr.$$

This configuration is tearing mode unstable for $\theta > 1.08$. Fig.3 shows the value of Δ' as a function of radius close to the marginal radius for $K = -0.60$ which can be used to calculate the growth rate in the limit of large S . The values obtained from equation (4) compare moderately well with results from resistive growth rate calculations. Fig.4 shows the marginal radial field perturbation as compared with a perturbation obtained from the growth rate calculation in which the full resistive set of equations is solved. In this case $S = 200$ so that the resistive layer thickness is an appreciable fraction of the radius and the agreement between the perturbations is not so good.

The tearing mode stability of the Bessel function model can be obtained analytically [36] as $\frac{d\sigma}{dr} = 0$ and equation (2) is not singular. The results differ little from the magnetohydrodynamic ones and give tearing mode stability

for $\theta < 1.56$. This configuration possesses a reverse field for $\theta > 1.2$ and is a minimum energy state [16].

In the past a variety of reverse field pinch configurations have been generated by choosing the quantity $P = \frac{rB}{B_\theta}$ to be a simple analytic function for example $P = 4e^{-r^2/\lambda_1} - 2$ with $\lambda_1 = 3 \rightarrow 20$. The curvature of the pitch, P , on axis is $\gamma = -8/\lambda_1$. For $\lambda_1 = 3$ the resultant field configuration obtained is completely stable magnetohydrodynamically for $r < 2.31$ with a central value of β of 31% [5]. This configuration violates the on axis tearing mode criterion, equation (8), for both $m = 1$ and $m = 2$ modes. The resultant tearing mode stability diagram is shown in Fig. 5. The position of the singularity for $m = 1$ and 2 is shown and that for $m = 0$ indicated by an arrow. All three modes are unstable though the $m = 0$ mode is stabilised by moving the conducting wall in from the position giving ideal magnetohydrodynamic stability. As the wavenumber approaches the value which gives a singularity on axis so the $m = 1, 2$ radial field perturbations become progressively localised in this region. A typical perturbation for $m = 0, 1$ and 2 is shown in Fig. 6. For $\gamma = -8/3$ the behaviour of the $m = 1$ and $m = 2$ tearing modes arising from the violation of the stability criterion influences the full radius of the pinch, Fig. 6. As γ approaches $-4/5$ for $m = 1$ and $\gamma = -4/3$ for $m = 2$ so the modes become highly localised on axis which would presumably not be serious in a real situation, indeed the growth rate calculations show this to be the case.

Our calculation predicts the disappearance of the on-axis mode for $m = 1$ as $\lambda_1 > 10$ i.e. $\gamma = -4/5$ and furthermore the calculated value of $r_S \Delta'$ for small r_S is in good agreement with equation (6) (for example for $m = 1$, $\lambda_1 = 6$ we obtain $r_S \Delta' = 6.67$ compared with 6.70, for $r_S = 0.055$, from equation (6)).

V. Tearing mode stable reverse field pinches

Armed with the knowledge about the on axis behaviour and the properties of the Bessel function model we can then attempt to construct configurations in which $\sigma(r)$ becomes small or zero in the outer regions of the pinch but is approximately constant in the central region. This can be achieved by

expanding $P(r)$ as

$$P(r) = 2 \left(1 - \frac{r^2}{8} - \frac{r^4}{\lambda} - \frac{r^6}{\delta} - \frac{r^8}{\epsilon} \dots \right) \dots (19)$$

which has $\gamma = -\frac{1}{2}$ and therefore satisfies the on axis criterion. If $\lambda = 192$ then the configuration matches the Bessel function model to terms of order r^4 . The procedure is then to vary λ , δ , ϵ to obtain the maximum radius for stability for both $m = 0, 1$ for all values of K . Some examples will illustrate the general features in attempting to 'optimise' a reverse field pinch. The tearing mode stability diagram for $\lambda, \delta, \epsilon \rightarrow \infty$ is given in Fig. 7. This particular configuration has $P \propto r^2$ at large radii and therefore possesses vacuum fields as $r \rightarrow \infty$. The diagram is characterised by three unstable regions. An $m = 1$ region with $K < 0$ arising from tearing modes originating in the core of the plasma. An $m = 0$ region which is most unstable for $K \rightarrow 0$, arising from the field reversal point - marked with a dotted line. The growth rate for the $m = 0$ mode is a maximum for $K \neq 0$ and is actually zero for $K = 0$ (equation (4)). The third region is for $m = 1$ with $K > 0$ which is a result of tearing modes and MHD kinks arising in the outer regions of the plasma. In this case for $K < 0.2$ the modes are MHD kinks and for $K > 0.2$ tearing modes. This particular configuration is most unstable to an internal tearing mode and requires $\theta < 1.38$ for stability. The axial field is barely reversed at the conducting wall in this case.

For $\lambda = 192$, but $\delta, \epsilon \rightarrow \infty$ the position is somewhat improved. The internal tearing mode is now stable and the configuration is unstable to $m = 1$ tearing modes arising in the outer regions for $\theta > 2.8$ as shown in Fig. 8.

The optimum configuration obtained by varying λ appears to be when $\lambda = 400$ as shown in Fig. 9. Increasing λ still further makes the internal tearing mode more unstable. Decreasing λ makes the external $m = 0$ and $m = 1$ more unstable. The configuration is therefore tearing mode stable for $\theta < 3.7$, and the fields for this case are shown in Fig. 10. The current density at the marginal conducting wall position in this case is 5% of that on axis. Values of Δ' for $m = 1$ $K = -0.61$ and $m = 0, K = 0.3$ are shown in Fig. 11. Note that they are one order of magnitude smaller than those for the paramagnetic model shown in Fig. 3, indicating the greater stability that this configuration possesses.

Attempts were then made to modify this configuration so that it possessed a true vacuum edge region and with the current and current gradient[37] going to zero smoothly at the edge of the plasma. This was initially achieved by varying δ and ϵ in equation (19) but in no case could stability be achieved at a radius even approaching the vacuum edge of the plasma. It is apparent that the overall stability is very sensitive to $\frac{d\sigma}{dr}$ and the vacuum edge requires $\sigma > 0$ at this position so the gradient is increased and this tends to destabilise the original configuration.

Varying λ , δ , ϵ allowed us to search for an optimum and the results for the near optimum case are shown in Fig. 12. For a vacuum edge $R_v = 3.4$ the marginal stability curve for $m = 0$ almost reaches a radius of 3.4. For the edge at $R_v = 3.6$ the $m = 0$ mode is unstable. We can therefore conclude that it might be possible for the current to go to zero at the conducting wall and still retain stability. One should note that the $m = 1$ tearing modes arising from the outer region are affected by the attempt to produce a vacuum edge in that wave numbers greater than 1.0 are now unstable which is not the case for any of the previously quoted results (e.g. Fig. 8 or 9).

A somewhat more elaborate attempt to obtain a stable vacuum region was made by expanding the azimuthal current in the vicinity of the vacuum edge as

$$J_\theta = \mu x^2 + \nu x^3 + \phi x^4$$

where $x = R_v - r$ and R_v is the vacuum edge, and then matching the fields and gradients at another radius r_m to determine μ , ν , ϕ in terms of the previously calculated fields based upon equation (19). The matching zone size, $R_v - r_m$, is then also used as a variable. If the matching zone is too small it creates its own tearing modes because $\frac{d\sigma}{dr}$ is made too large. For $R_v = 4.0$ and a zone size of 0.75 complete stability is obtained for radii less than 4.11 representing a vacuum region of 2.8% of the radius and this is shown in Fig. 13. There are now four unstable regions produced by the configuration, the new region for wavenumbers of ~ 0.5 is produced by the matching zone. Optimisation now consists of varying R_v and r_m such that the four unstable regions have their minimum radii maximised. In practice only two of the zones prove to be troublesome, the one

associated with $m = 0$ and that arising from the matching zone for $m = 1$. Fig.14 demonstrates this optimisation for a zone size of 0.9. The $m = 0,1$ stability boundaries are shown as a function of R_v and the percentage vacuum obtained. The result is that complete tearing mode stability is possible with a vacuum region of $< 4\%$ in radius.

VI. The stability of such field configurations at finite β

It has already been established that reverse field pinch configurations can be magnetohydrodynamically stable at high β . Values of 30% can be readily obtained [5] and optimisation shows that values of 60% are possible [18]. It is also known that the Bessel function model modified to include a pressure gradient can confine a β of 27% with the conducting wall on the plasma [18]. The method of introducing the pressure gradient in the latter model is not unique so the value only typifies what is possible.

For these configurations defined by the pitch given in equation (19) we can generate a pressure gradient locally by permitting it to approach that value given by the Suydam criterion using the shear associated with the given pitch but with a multiplicative factor less than unity. It is then possible to explore the ideal hydromagnetic β limitations of the tearing mode stable reverse field pinches by varying this factor. For $\lambda = 400$, $\delta, \epsilon \rightarrow \infty$ using the Newcomb analysis we find that the maximum β is 17% for a pinch configuration parameter, θ , of 3. The behaviour of β with θ is shown in Fig.15. For the configuration with a vacuum region of 4% in radius the maximum value of β is 12% for a pinch parameter, θ , of 2.5.

To determine the effect of the pressure gradient on the tearing modes we have used an initial value calculation [13] to obtain the growth rates. This is always found to be destabilising and the value of β for the configuration without a vacuum edge is reduced to about 12% and the value of θ to around 2.0. It must be noted that such configurations would be unstable to the localised resistive interchange mode [27,43] though finite larmor radius effects may stabilise such instabilities.

We would therefore conclude that the above reverse field pinch configurations can be grossly stable to both ideal and resistive tearing modes at values of β up to about 12%.

VII. Discussion

We have demonstrated that there exists a class of reverse field pinch configurations which are tearing mode stable at zero β . These configurations can possess a small vacuum region between the plasma and conducting wall. The conducting wall is necessary to give stability to $m = 0$ and $m = 1$ instabilities.

Evidence for tearing modes in tokamaks is now very good and their detailed structure has been obtained from soft X-ray emission measurements from the region of the singular surfaces [40] and from magnetic probes [38,39]. Similar modes may also be present in screw pinches [41]. Tearing modes are more difficult to detect in pinches because ordinary MHD kink modes appear under rather similar conditions. However detailed studies with probes on the high β experiment at Culham [7] have revealed the presence of the $m = 1$ tearing mode which was found to be in reasonable agreement with the predictions of a growth rate calculation including not only the resistivity but other dissipative effects.

In slow pinch experiments such as Zeta relatively stable or quiescent operation was demonstrated for pinch configuration parameters between 1.2 and 2.5 [42]. Under these conditions a reverse field was present. In this experiment the metal liner acted as a relatively good conducting wall to possible $m = 0$ instabilities and the conducting shell was about 10% in radius away from the edge of the plasma. These observations would appear to be in reasonable agreement with the tearing mode stable configurations that we have obtained here where the stability window for a vacuum edge is $1.2 < \theta < 2.7$.

The behaviour of slow pinch experiments can be understood in terms of resistive instabilities permitting the pinch to relax by field line reconnection to the minimum energy configuration of Taylor. However the constraints in the outer regions of the pinch are such as to limit the current flow in that region and produce significant departures from that state. We have demonstrated that such a constraint is compatible with a tearing mode stable reverse field pinch.

VIII. Conclusions

1. Tearing mode stable reverse field pinch configurations have been obtained which in the central regions of the pinch are of the form given by Taylor and in the outer regions carry little or no current.
2. Stability at zero β is possible with a small vacuum region outside the pinch.
3. The conducting wall plays a vital role in stabilising both the $m = 0$ and $m = 1$ instabilities which arise in the core and in the outer regions of the plasma.
4. A stability criterion is obtained for the central regions of a cylindrical pinch from which it is deduced that the current must be peaked on axis.
5. Stable configurations at zero β exist with a pinch configuration parameter, θ , up to 3.5 which permit strong ohmic heating.
6. Such configurations are stable to ideal hydromagnetic instabilities for central values of β of $\leq 17\%$.

Acknowledgements

I would like to thank B Bernardo and P Ingram of Hatfield Polytechnic, London, for assisting in the development of the numerical code and A S Furzer of Royal Holloway College, University of London, for the resistive growth rate calculations at finite β .

References

- [1] TAYLER, R.J., Proc. Phys. Soc.Lond. B70, 1049, 1957.
- [2] ROSENBLUTH, M.N., Int. Conf. on Peaceful Uses of Atom. Energy, Geneva, Vol. 31, 85, 1958.
- [3] KADOMTSEV, B.B., Review of Plasma Physics, Consultants Bureau, New York, Vol.5, p.268, 1970.
- [4] SHAFRANOV, V.D., Zh. Tek. Fiz. 40, 241, 1970.
- [5] ROBINSON, D.C., Plasma Physics 13, 439, 1971.
- [6] SCHUURMAN, W., et al., Plasma Physics, 11, 495, 1969.
- [7] BUTT, E.P. et al., 5th Conference on Plasma Physics and Controlled Nuclear Fusion, Tokyo, Vol.3, 417, 1975.
- [8] FURTH, H.P., RUTHERFORD, P.H., SELBERG, H. Phys. Fluids 16, 1054, 1973.
- [9] HOSEA, J.C., et al., 4th Conference on Plasma Physics and Controlled Nuclear Fusion, Madison, Vol.2, 425, 1971.
- [10] GLASSER, A.H., GREENE, J.M., JOHNSON, J.L., Phys. Fluids 19, 567, 1976.
- [11] FURZER, A.S., ROBINSON, D.C., 7th European Conference on Controlled Fusion and Plasma Physics, Vol.1, p.113, Lausanne, 1975.
- [12] DOBROTT, D., PRAGER, S.C., TAYLOR, J.B., Culham Laboratory Report, CLM-P486, 1977.
- [13] CROW, J.E., KILLEEN, J., ROBINSON, D.C., 6th European Conference on Controlled Fusion and Plasma Physics, Moscow, 269 1973.
- [14] DIBIASE, J.A., Lawrence Livermore Laboratory, UCRL-51591, 1974.
- [15] KADOMTSEV, B.B., 6th Conference on Plasma Physics and Controlled Nuclear Fusion, Berchtesgaden, Vol.1, 555, 1977.
- [16] TAYLOR, J.B., 5th Conference on Plasma Physics and Controlled Nuclear Fusion, Tokyo, Vol.1, 161, 1975.
- [17] ZUEVA, N.M., SOLOV'EV, L.S., MOROZOV, A.I., Letters to Zh. Ehksp. Teor. Fiz. 23, 284 1976.
- [18] GOWERS, C.W. et al., 6th Conference on Plasma Physics and Controlled Nuclear Fusion, Berchtesgaden, Vol.1, 429, 1977.

- [19] WHITE, R.B., et al., Physics Fluids, 20, 800, 1977.
- [20] GLASSER, A.H., FURTH, H.P., RUTHERFORD, P.H., Phys. Rev. Letters 38, 234, 1977.
- [21] ROBINSON, D.C., Bull. Am. Phys. Soc. 20, 1297, 1975.
- [22] ROBINSON, D.C., 3rd Topical Conf. on High Beta Plasmas, Culham, Pergamon Press, p.273, 1976.
- [23] NEWCOMB, W.A., Annals of Physics, 10, 232, 1960.
- [24] KADOMTSEV, B.B., Nuclear Fusion Suppl. 3, 969, 1962.
- [25] FURTH, H.P., KILLEEN, J., ROSENBLUTH, M.N., Phys. Fluids 6, 459, 1963.
- [26] JOHNSON, J.L., GREENE, J.M., COPPI, B., Phys. Fluids 6, 1169, 1963.
- [27] COPPI, B., GREENE, J.M., JOHNSON, J.L., Nucl. Fusion 6, 101, 1966.
- [28] ROBINSON, D.C., 2nd Symposium on Toroidal Plasma Confinement, Dubna, 1969, Culham Laboratory CLM-R 150.
- [29] PAPALOIZOU, J., private communication.
- [30] HAMMING, R.W., Numerical Methods for Scientists and Engineers, New York, McGraw Hill, 1962.
- [31] DIBIASE, J.A., KILLEEN, J., J. Computational Phys. Vol.24, p.158, 1977.
- [32] ROBINSON, D.C., 3rd Symposium on Plasma Heating in Toroidal Devices, Varenna, p.168, 1976.
- [33] BICKERTON, R.J., Proc. Phys. Soc. London B22, 618, 1958.
- [34] WHITEMAN, K.J., Plasma Phys. 7, 293, 1965.
- [35] BURTON, W.M., et al., Nucl. Fusion, Suppl. 3, 903, 1962.
- [36] GIBSON, R.D., WHITEMAN, K.J., Plasma Phys. 10, 1107, 1968.
- [37] WESSON, J.A., Proc. 7th European Conf. on Controlled Fusion and Plasma Physics, Lausanne, Vol.II, 102, 1975.
- [38] TOYAMA, H., et al., 6th Conf. on Plasma Physics and Controlled Nuclear Fusion, Berchtesgaden, Vol.1, 232, 1977.
- [39] ROBINSON, D.C., - submitted to Phys. Rev. Letters.
- [40] VON GOELER, S. Proc. 7th European Conf. on Controlled Fusion and Plasma Physics, Lausanne, Vol.II, 71, 1975.

- [41] MIMURA, M., KOOIKMANN, W., OOMENS, A.A.M., Rijnhuizen Report 76-99, 1976.
- [42] ROBINSON, D.C., KING, R.E., Proc. 3rd Conf. on Plasma Physics and Controlled Nuclear Fusion, Vol.1, p.263, IAEA Vienna, 1968.
- [43] ROBINSON, D.C. Proc. 8th European Conference on Controlled Fusion and Plasma Physics, Prague, 1977.

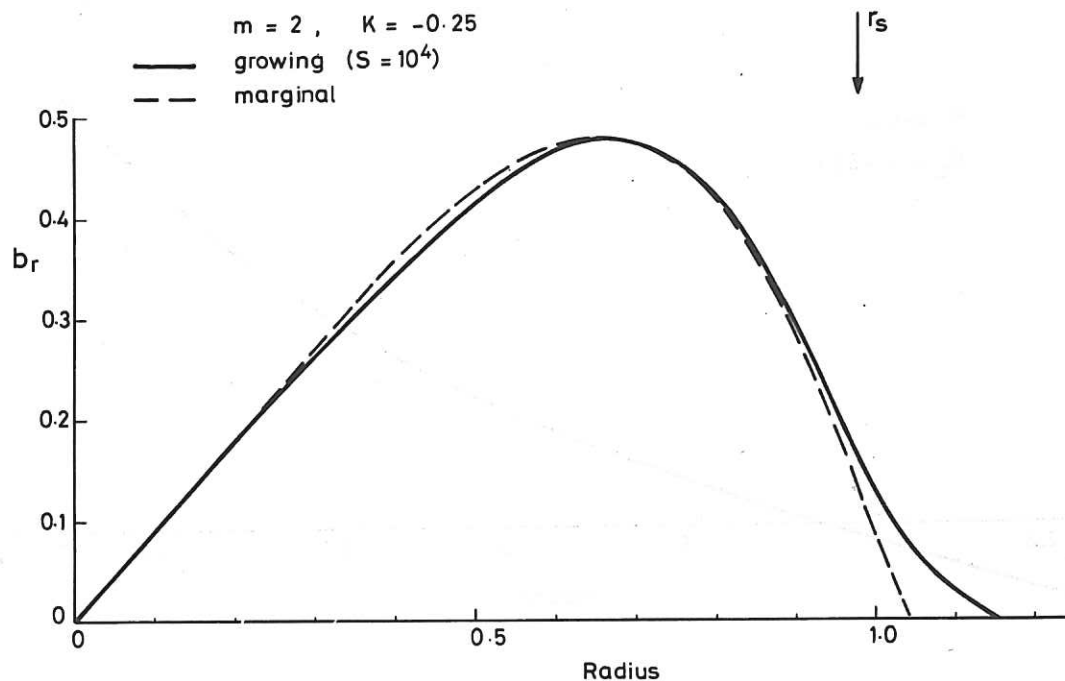


Fig.1 Radial field perturbations from the marginal stability calculation and for a growing mode near marginal stability for $m=2$ and current distribution with $J_z = J_0 (1 - r^4)^2$.

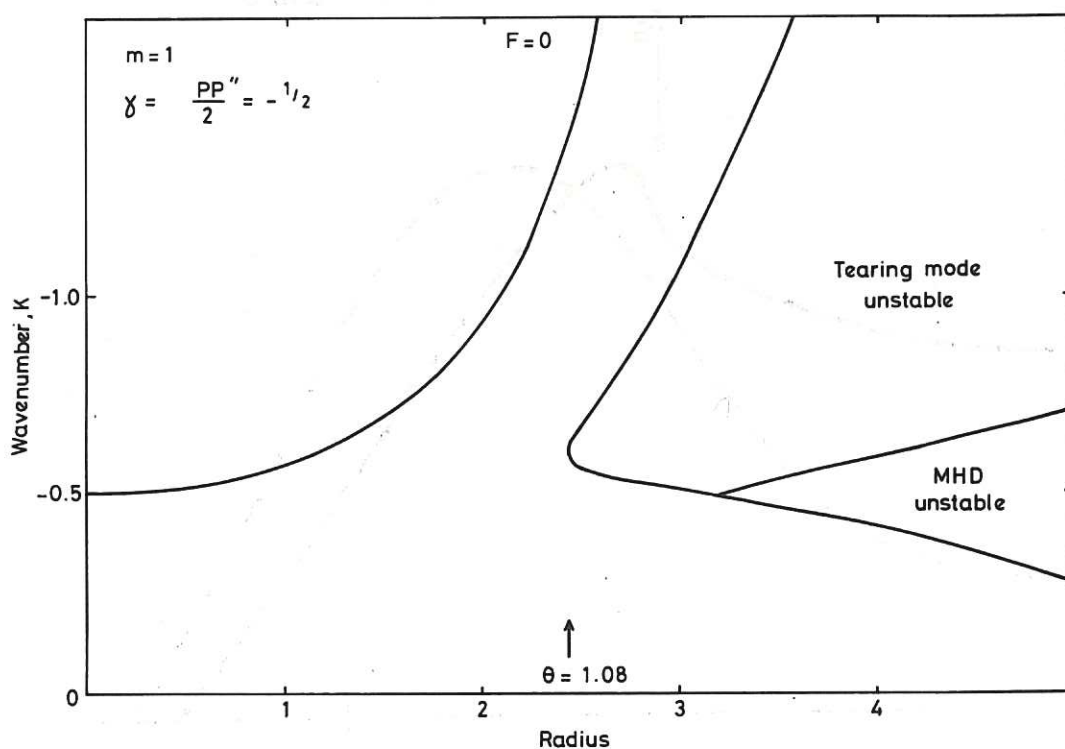


Fig.2 Marginal stability diagram for the force-free paramagnetic model. The marginal stability curves for the $m=1$ tearing mode and MHD kink mode in the wavenumber, K , normalised radius plane are shown. The position of the singular surface is shown by the $F=0$ curve.

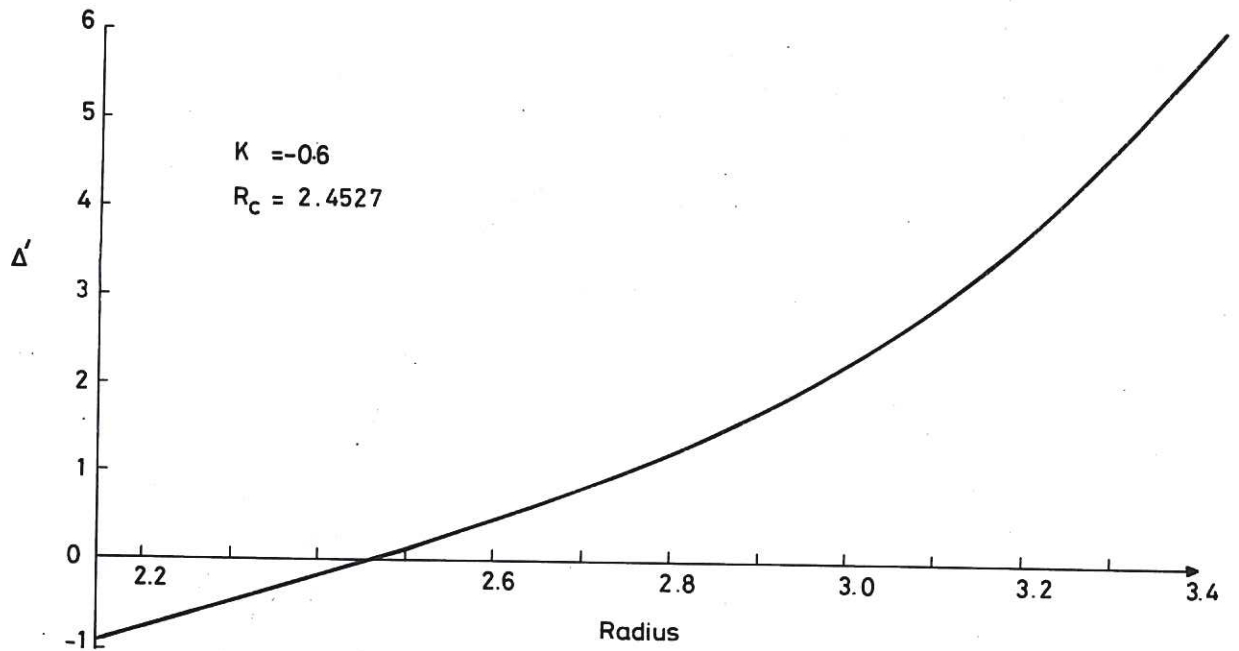


Fig.3 Δ' as a function of normalised radius for the force-free paramagnetic model for $m = 1$ and $K = -0.60$.

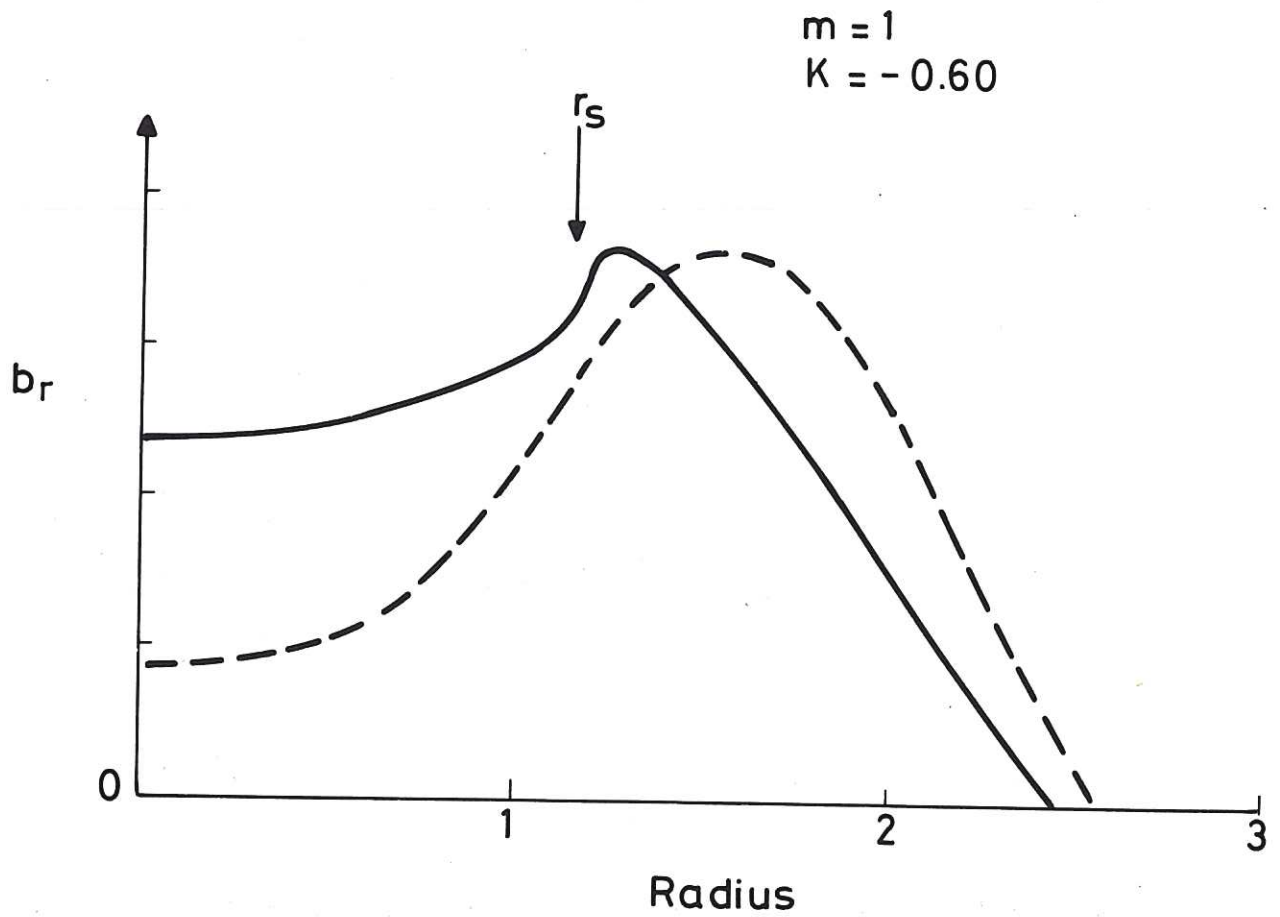


Fig.4 Radial field perturbations for the force-free paramagnetic model from the marginal stability, —, and growth rate, ---, calculations for $m = 1$, $K = -.60$.

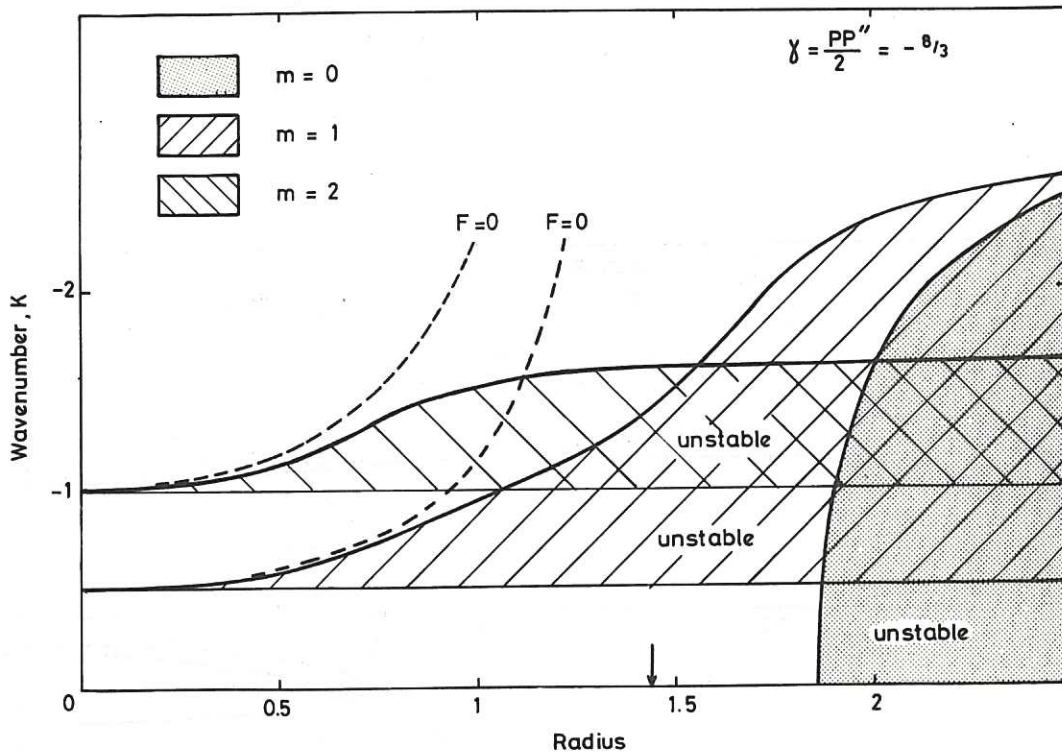


Fig.5 Marginal stability diagram for resistive modes for an MHD stable reverse field pinch configuration with $\gamma = -8/3$. Unstable regions for $m = 0, 1, 2$ are shown as are the positions of the singular surfaces $F = 0$ for $m = 1$ and $m = 2$. The position for the singular surface for $m = 0$ is indicated by the arrow. The MHD unstable region occurs only for K positive and $r > 3.0$.

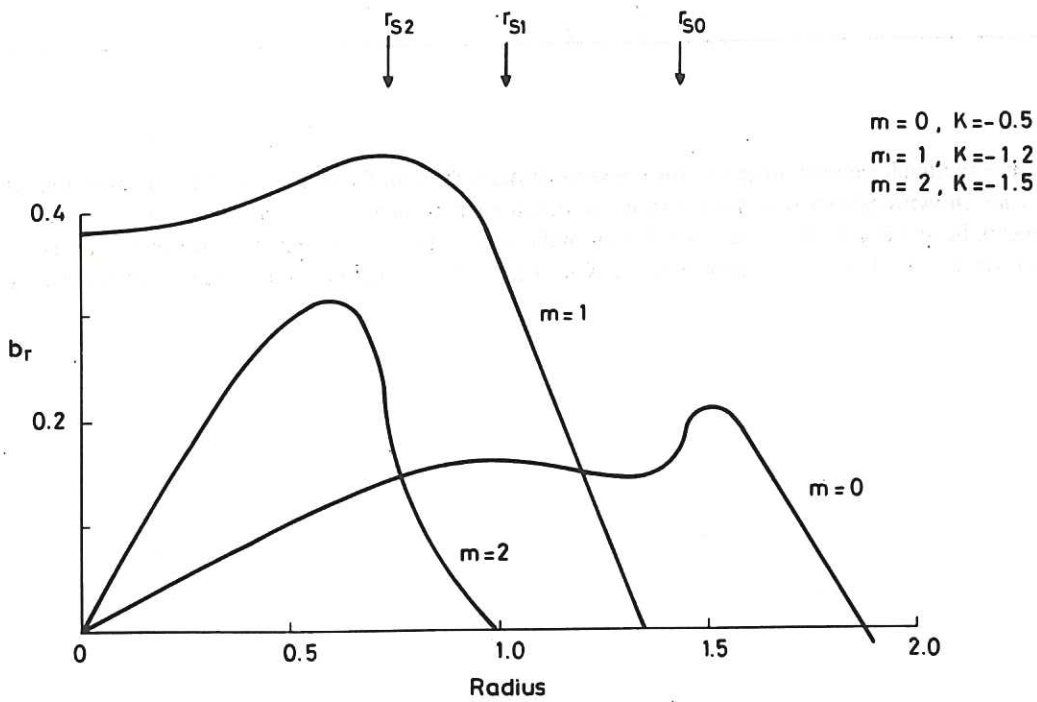


Fig.6 Radial field perturbations for the MHD stable reverse field pinch for $m = 0, K = -0.5$, $m = 1, K = -1.2$, and $m = 2, K = -1.5$. r_{s0}, r_{s1}, r_{s2} indicate the positions of the singularities for $m = 0, 1$ and 2 respectively.

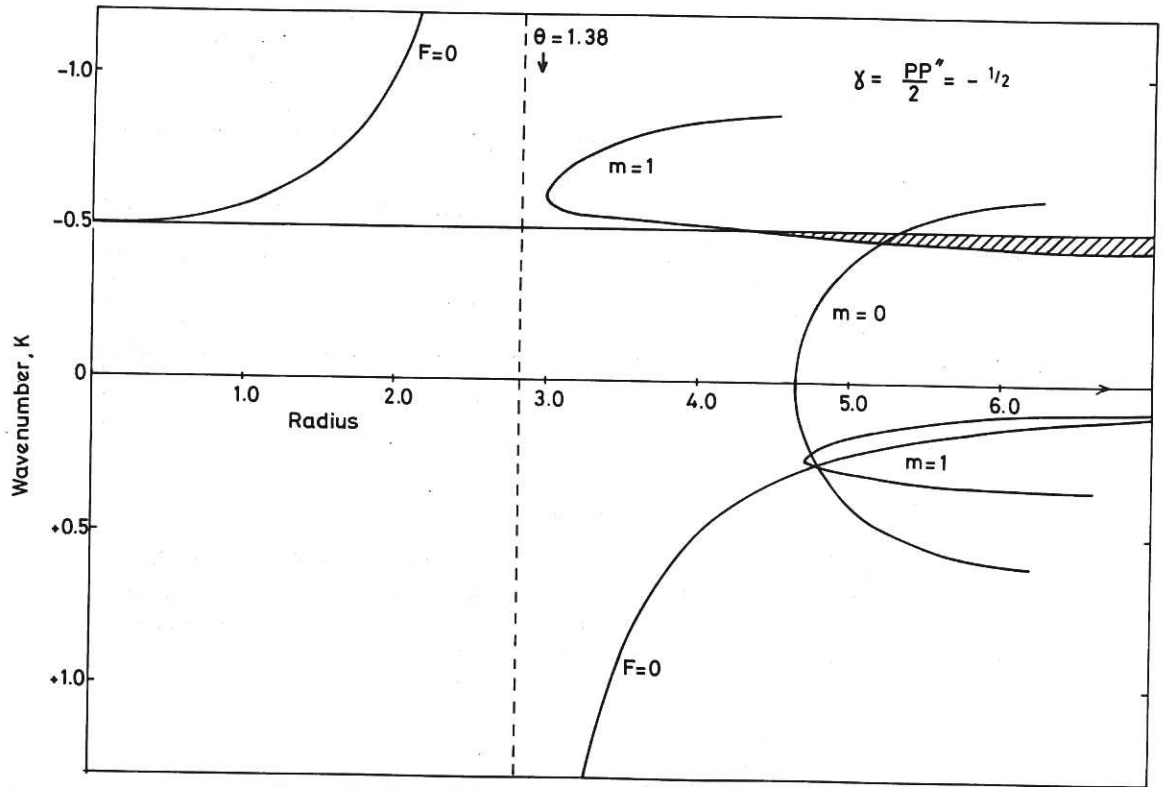


Fig.7 Resistive marginal stability diagram, for a reverse field pinch with $P(r) = 2(1 - r^2/8)$. Unstable regions for $m = 0, 1$ are shown together with the positions of the singular surfaces. The maximum value of θ for which there can be stability in this case is $\theta = 1.38$ as indicated. The hatched region shows an MHD unstable region for $K < 0$, there is also one for $m = 1$, $K < 0.25$. The dotted line indicates the radius at which $B_z = 0$.

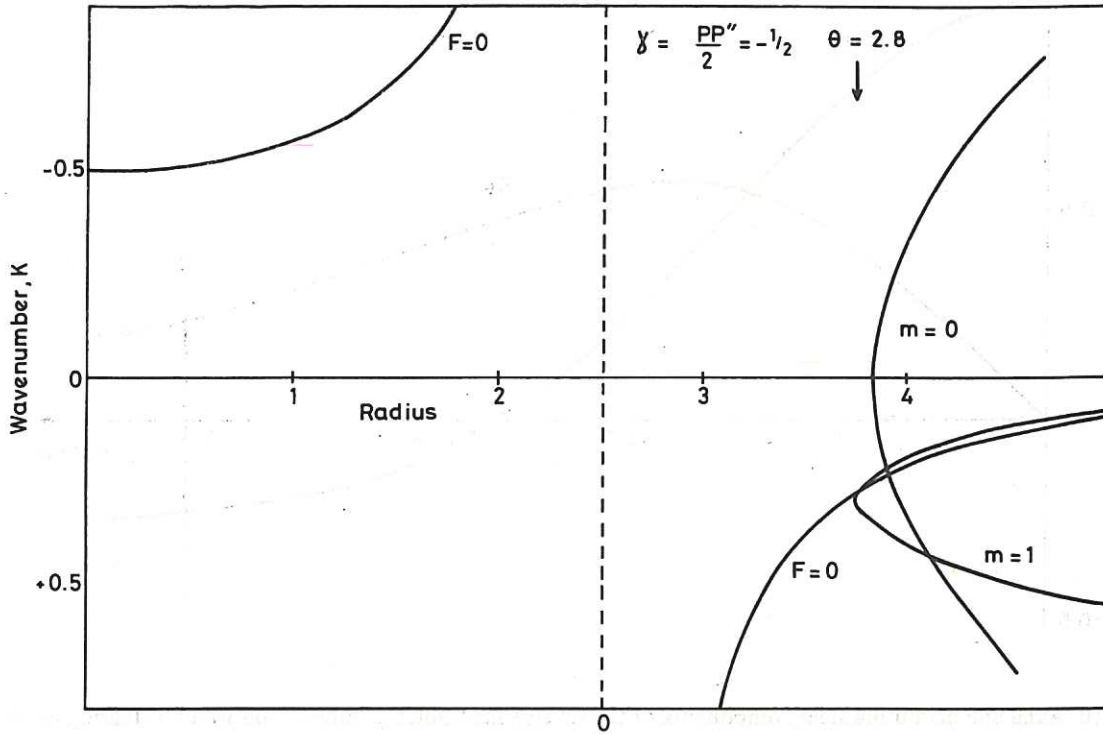


Fig.8 Marginal stability diagram for a reverse field pinch with $P(r) = 2(1 - r^2/8 - r^4/192)$. The configuration is unstable to the right of marginal stability curves shown for $m = 0, 1$. The maximum value of θ in this case is 2.8.

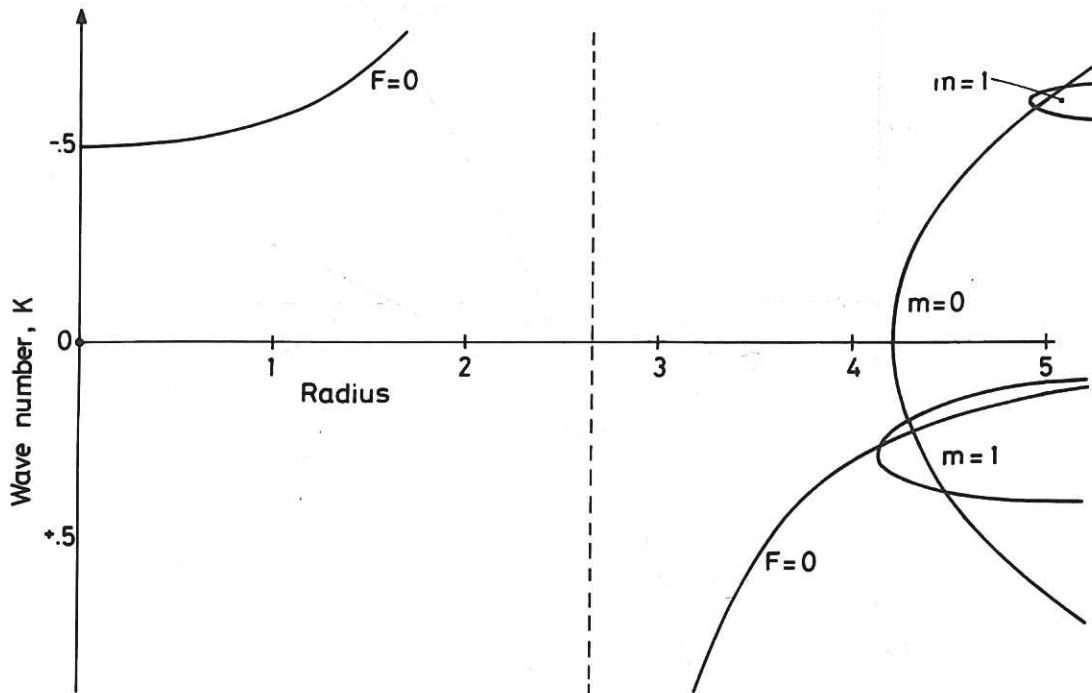


Fig.9 Marginal stability diagram for a reverse field pinch with $P(r) = 2(1 - r^2/8 - r^4/400)$ and giving tearing mode stability for $\theta < 3.7$.

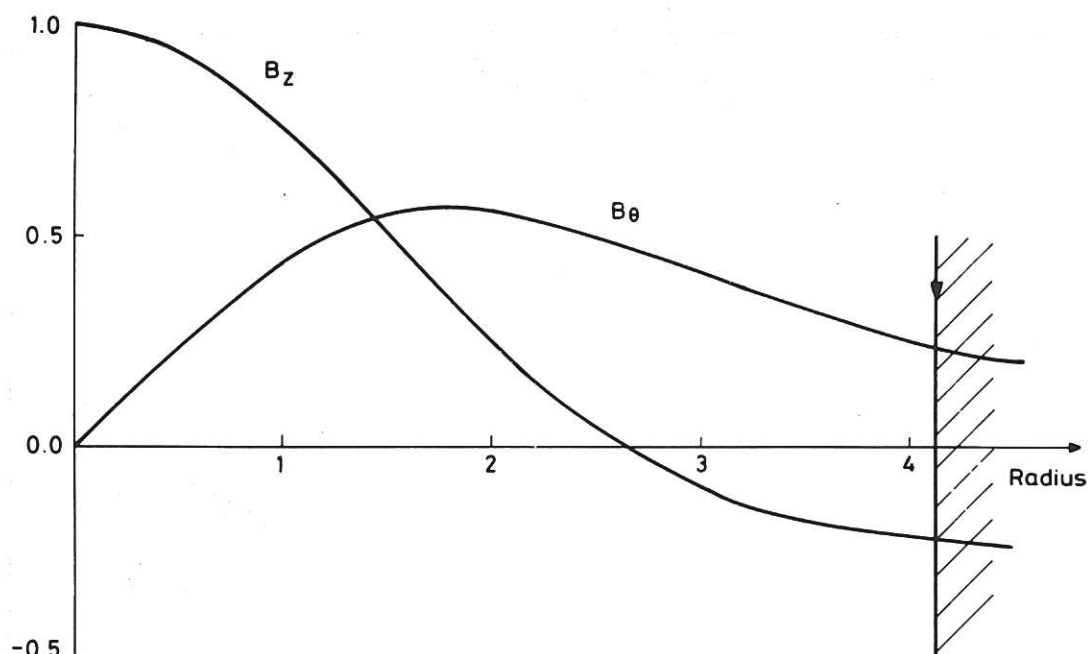


Fig.10 Axial and azimuthal field components of the reverse field pinch configuration which is tearing mode stable for $\theta < 3.7$. The maximum radial position for a conducting wall to give stability is indicated.

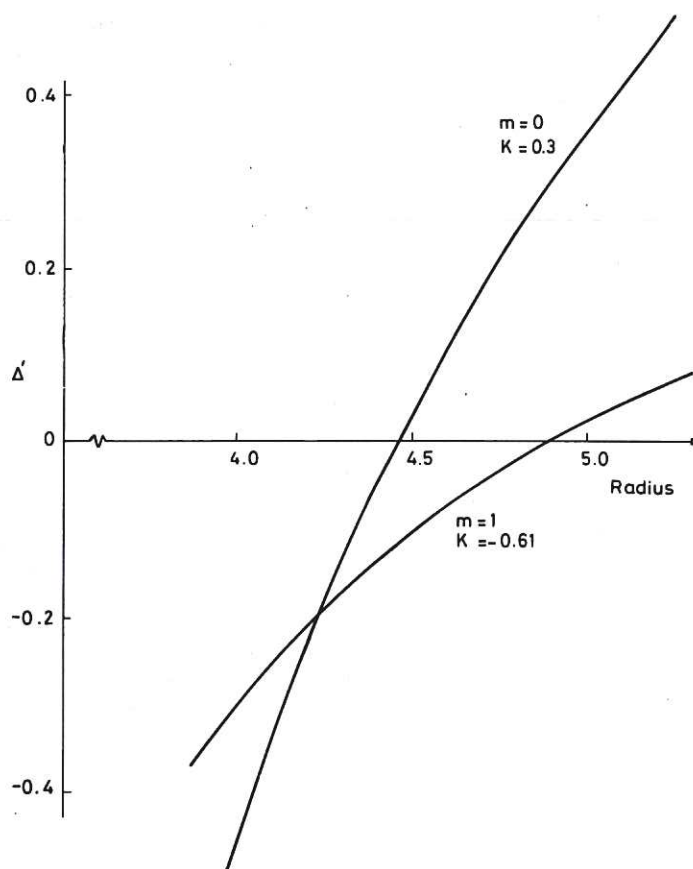


Fig.11 Values of Δ' for the reverse field pinch configuration shown in Fig.9 for $m = 1$, $K = -0.61$ and $m = 0$, $K = +0.3$.

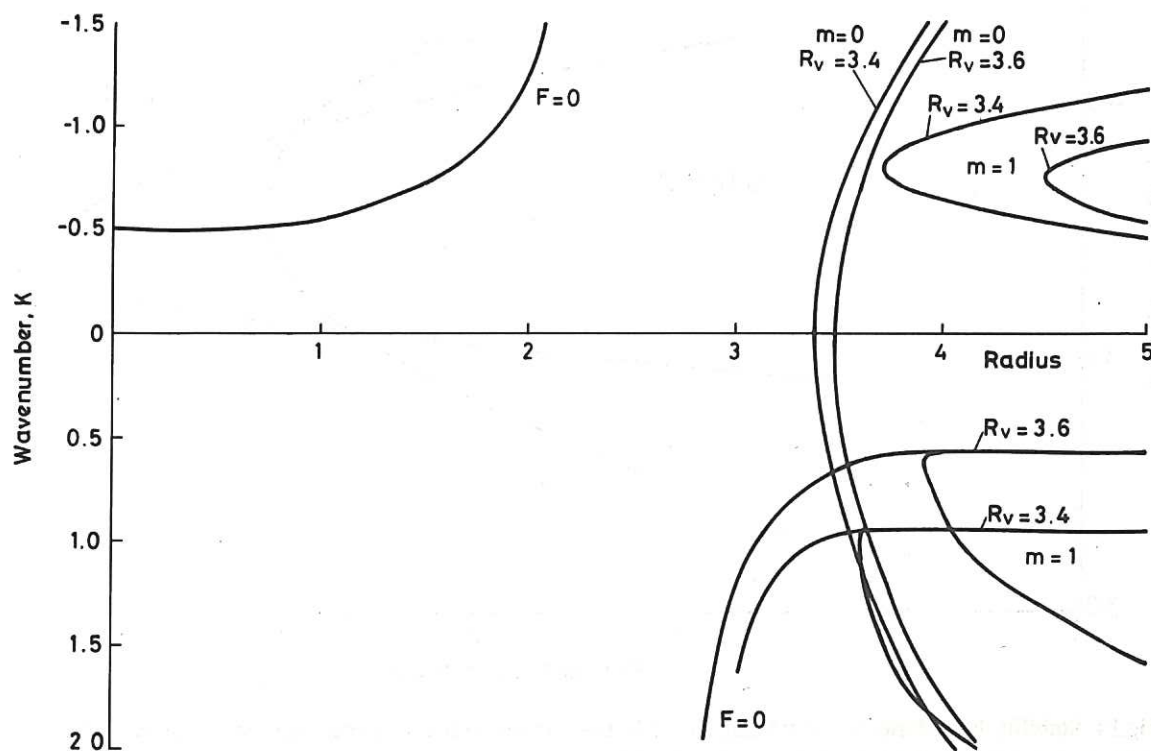


Fig.12 Stability diagram for the reverse field pinch of Fig.9 modified to have a vacuum edge at a radius of either $R_v = 3.4$ or $R_v = 3.6$. The singular surface for $m = 1$ in the core does not change for the two configurations but it does in the outer regions so two curves are shown for $K > 0$.

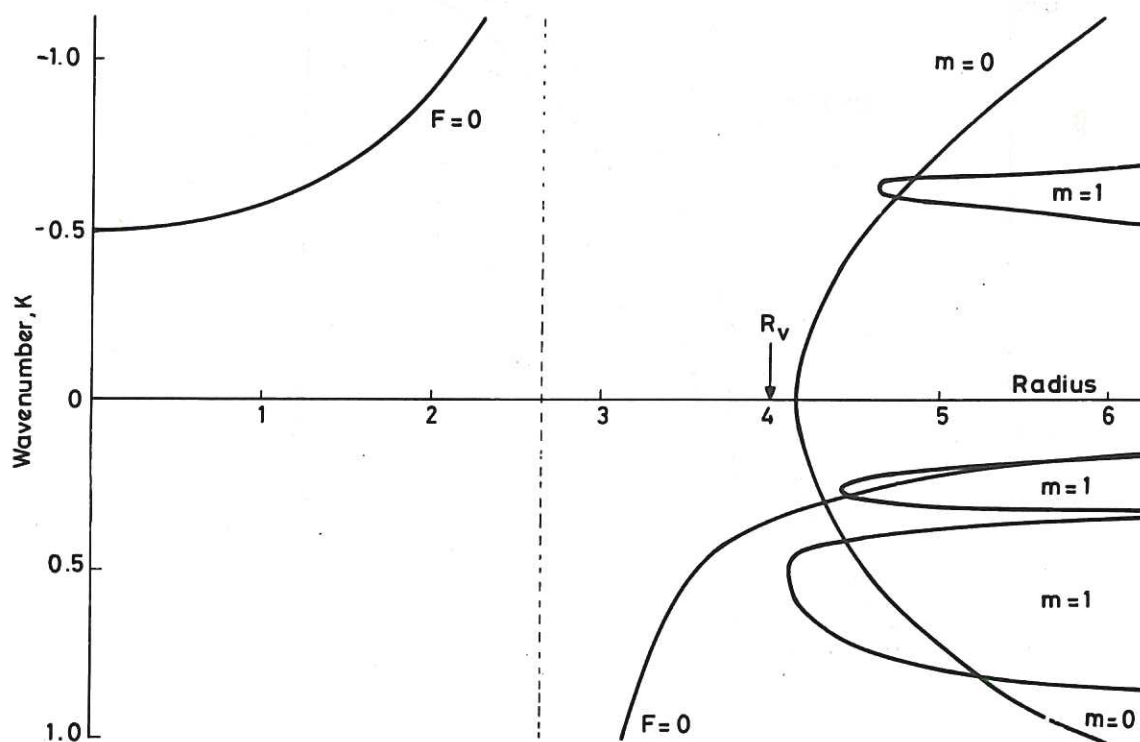


Fig.13 Stability diagram for a reverse field configuration based upon Fig.9 but with a vacuum matching zone from 3.25 to 4.0 and a vacuum for $r > 4.0$. The configuration is unstable to the right of the four marginal stability curves shown for $m = 0, 1$.

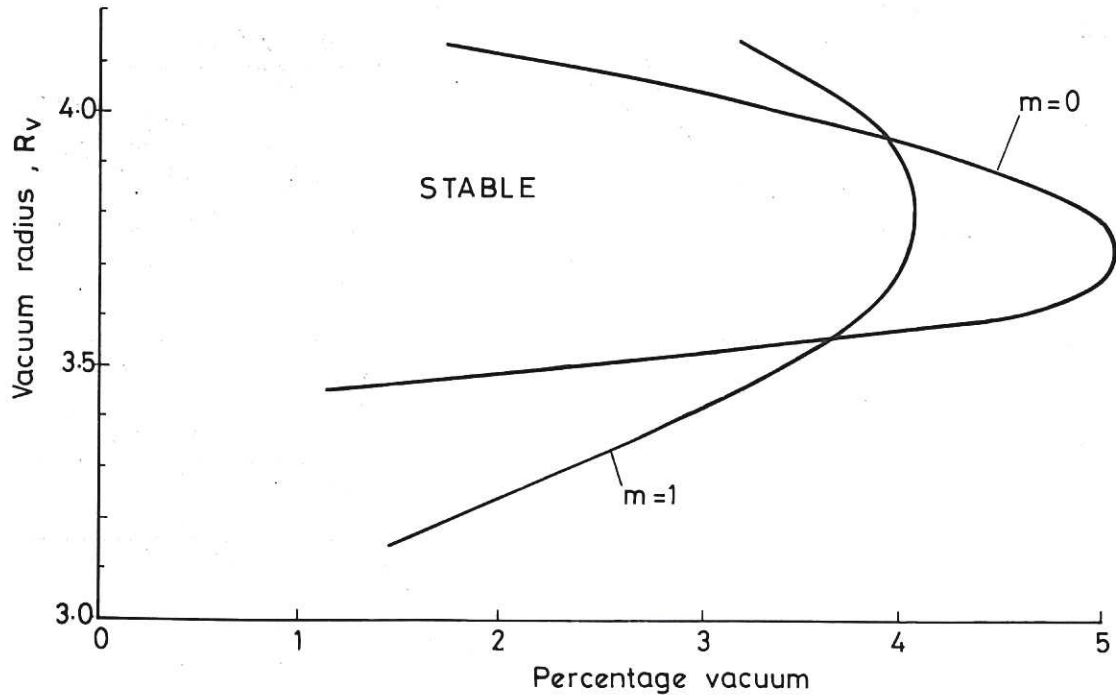


Fig.14 Stability boundaries for $m = 0$ and $m = 1$ in the vacuum radius – percentage vacuum plane. A stable region exists to the left of the curves. In this case the matching zone size was 0.9.

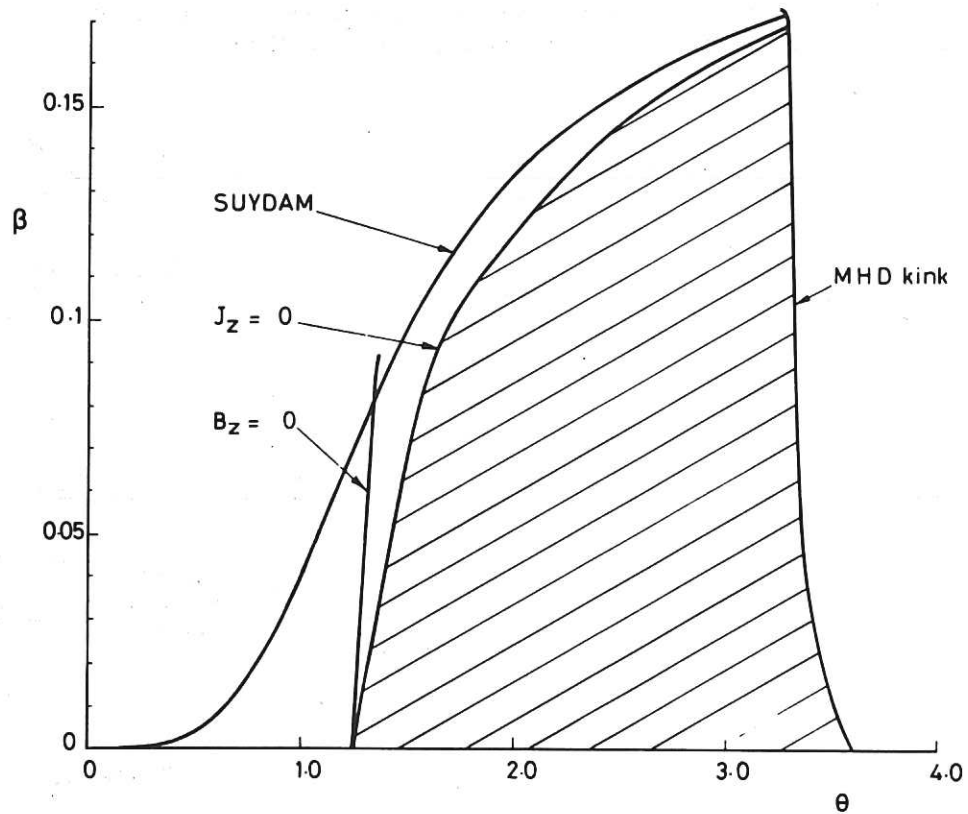


Fig.15 Central value of β as a function of θ for a tearing mode stable reverse field pinch configuration. The curve on the right is obtained from the Newcomb analysis and the upper curve from the Suydam criterion. The other two curves gives the conditions $B_z = 0$, $J_z = 0$. The hatched region is MHD stable with a small vacuum region.

